The International Journal of Advanced Manufacturing Technology (2022) 118:1227–1238
https://doi.org/10.1007/s00170-021-08015-0

ORIGINAL ARTICLE

Dual-frequency ultrasonic cleaning with diluted phosphoric acid solution for removing oxide scale of uncoated steel sheets in hot stamping

Naotaka Nakamura[1] · Ken-ichiro Mori[1] · Tsuyoshi Komatsu[1] · Takafumi Hayashi[2] · Takayuki Suzuki[3] · Tadashi Okazaki[4] · Yohei Abe[1]

Received: 31 May 2021 / Accepted: 5 September 2021 / Published online: 15 September 2021

Abstract

Dual-frequency ultrasonic cleaning with a diluted phosphoric acid solution was developed to remove oxide scales on surfaces of hot-stamped parts from uncoated steel sheets, and conventional shot blasting processes are omitted. The removal of the oxide scale by ultrasonic cleaning is accelerated by the phosphoric acid solution and the dual frequency. The removing time for the phosphoric acid solution was shorter than that for a hydrochloric acid solution, and rust appearing for leaving after cleaning was prevented by generating an iron phosphate layer. In dual-frequency ultrasonic cleaning with the diluted phosphoric acid solution, the oxide scale was dissolved, and then the oxide scales were exfoliated from the thin scale and high-pressure portions. The removing time decreased with decreasing pH and oxide scale thickness and with increasing solution temperature. The surface roughness and distortion of an ultrasonic-cleaned hot-stamped part were smaller than those for shot blasting, and the weldability and paintability were similar. The oxide scale of a hot-stamped part having a nonuniform distribution of oxide scale thickness was successfully removed by dual-frequency ultrasonic cleaning with the diluted phosphoric acid solution.

Keywords Hot stamping · Uncoated steel sheet · Oxide scale · Ultrasonic cleaning · Phosphoric acid

1 Introduction

For lightweighting and high crash safety of automobiles, the application of ultrahigh-strength steel parts is useful [1]. In cold stamping of ultrahigh-strength steel sheets, large spring back [2], low formability [3], and low tool life [4] are problematic. To avoid these problems, ultrahigh-strength steel parts having a tensile strength of about 1500 MPa are commonly produced by hot stamping of quenchable steel sheets [5]. The sheets are heated to about 900 °C to be transformed into austenite, then are formed, and are die-quenched to be transformed into hard martensite. By heating the sheets, the forming load becomes small, and the ductility is improved. Furthermore, the spring back is considerably reduced by die quenching until a temperature below the martensite finish one [6].

To prevent the oxidation at high temperatures, Al-Si-coated steel sheets are mostly utilized for hot stamping [7]. In the Al-Si-coated sheets, slow heating of about 5 min is required to generate intermetallic compound layers for preventing the oxidation of surfaces. The length of the furnace becomes considerably long, 20–50 m, and increases with increasing shots per minute for presses. Although zinc-coated steel sheets are also used to prevent the oxidation in hot stamping, it is necessary that the heated zinc is appropriately solidified to prevent cracking induced by the liquid-metal embrittlement, and thus the productivity is low as well as the Al-Si-coated sheets [8]. To reduce the area of the furnace, compact multichamber furnaces with piled heating chambers were developed [9]. It is not easy to apply rapid heating such as resistance heating [10] and induction heating [11] to the Al-Si- and zinc-coated sheets. The weldability of hot-stamped parts from the coated

✉ Naotaka Nakamura
n_nakamura@plast.me.tut.ac.jp

[1] Department of Mechanical Engineering, Toyohashi University of Technology, Toyohashi, Aichi 441-8580, Japan

[2] Aisin Corporation, Kariya, Aichi 448-8650, Japan

[3] Aisin Takaoka Co., Ltd., Toyota, Aichi 473-8501, Japan

[4] Aisin Sin'ei Co., Ltd., Hekinan, Aichi 447-8508, Japan

sheets is not high. Particularly in projection welding of nuts, bolts, and positioning pins joined to the hot-stamped parts, welding spatter and failures are likely to occur because of the high electrical resistance and strength of the coating layer [12].

In uncoated steel sheets, the heating time is short, because only the austenite transformation is necessary without the temperature control of the coating layers. However, the uncoated sheets are considerably oxidized by heating to about 900 °C for the martensite transformation [13]. The oxidation is considerably decreased by a protective atmosphere such as nitrogen [14]. Since the hydrogen-induced embrittlement is problematic for the ultrahigh-strength steel parts [15], the nitrogen atmosphere has another advantage of the reduction in hydrogen diffusion at high temperatures. To prevent the oxidation of the uncoated sheets, Nano-X [16] and an oxidation preventive oil [17] were developed. The oxide scale of the hot-stamped parts from the uncoated sheets is generally removed by shot blasting to stabilize welding and painting [18]. In shot-blasted parts, not only rough surface but also distortion of thin parts is caused. Uncoating is suitable for development of new steel sheets such as 1800 MPa sheets [19], 2000 MPa sheets [20], and medium manganese sheets [21].

Ultrasonic cleaning is to remove contaminants adhering to metals, plastics, glass, and ceramics by means of cavitation bubbles [22]. In ultrasonic cleaning, a reentrant jet is generated by the collapse of the cavitation bubble and high-pressure acts on the surfaces of parts to be cleaned [23]. Goode et al. [24] applied ultrasonic cleaning using a diluted hydrochloric acid solution to remove the oxide scales of hot-rolled steel sheets. Maeno et al. [25] removed the oxide scales of hot-stamped uncoated steel sheets with ultrasonic cleaning using the diluted hydrochloric acid solution. Although the hydrochloric acid solution is effective in removing the oxide scale of steel, health and environmental problems are caused by the corrosive fog.

The phosphoric acid is widely used for surface treatments of steels. The zinc phosphate/stearate coatings are commonly employed for the lubrication in cold forging of steels under high pressure [26], and the paintability of electrodeposition coating is also improved [27]. The black phosphate coating with a thick layer and fine grains has high corrosion resistance [28]. The phosphoric acid has a rust conversion function for generating a proper painting layer by reaction with iron oxides [29] and has a function for removing oxide scales on steel surfaces [30]. The safety of the phosphoric acid is higher than that of the hydrochloric acid, and the dissolution rate of the oxide scale of steel for the diluted phosphoric acid is higher than that for the diluted hydrochloric acid [31].

In this paper, dual-frequency ultrasonic cleaning with a diluted phosphoric acid solution was developed to remove the oxide scale of uncoated steel sheets in hot stamping. The effects of dual-frequency ultrasonic cleaning and the phosphoric acid solution on the removal of the oxide scale were evaluated.

2 Ultrasonic cleaning with diluted phosphoric acid solution for removing oxide scale of hot-stamped parts

2.1 Dual-frequency ultrasonic cleaning

The oxide scales on surfaces of hot-stamped parts from uncoated steel sheets are removed by ultrasonic cleaning with a diluted phosphoric acid solution. The removal of the oxide scale by ultrasonic cleaning is accelerated by the phosphoric acid solution. In ultrasonic cleaning, the pressure acting on surfaces of a cleaned part becomes nonuniform [32], and thus the time for removing the whole scales increases. To reduce the removing time, dual-frequency ultrasonic cleaning was employed, as shown in Fig. 1. In conventional single-frequency ultrasonic cleaning, the pressure distribution depends on the wavelength of the ultrasonic wave because of the standing wave. The wavelength is calculated by dividing the velocity of the ultrasonic wave by the frequency. In the antinode portions located every half of the wavelength, the removing efficiency is high due to the high pressure, whereas the efficiency in the node portions is low due to the low pressure [33]. Although the cavitation effect is large for a low frequency [34], the pressure nonuniformity becomes remarkable. The tendency for a high frequency is opposite. In dual-frequency ultrasonic cleaning mixing the low and high frequencies, the standing wave is avoided, and in addition, the cavitation effect is enhanced in comparison with single-frequency ultrasonic cleaning [34]. The effect of dual-frequency ultrasonic cleaning on the removal of the oxide scale was examined.

2.2 Procedure of ultrasonic cleaning

The conditions of ultrasonic cleaning with the diluted phosphoric acid solution are given in Fig. 2. Each transducer oscillates at both low frequency of 28 kHz and high frequency of 75 kHz and has a function for adjusting the percentage of the two frequencies. The low frequency percentage f is defined by

$$f = P_{\mathrm{L}}/(P_{\mathrm{L}} + P_{\mathrm{H}}), \tag{1}$$

where P_{L} is the power of the low frequency and P_{H} is the power of the high frequency. The total power of the two frequencies of the equipment was fixed at 300 W. The power of the low frequency was limited to 150 W; i.e., the low frequency percentage ranges between 0 and 50%. The phosphoric acid was diluted with water to pH 1 and 2. The temperatures

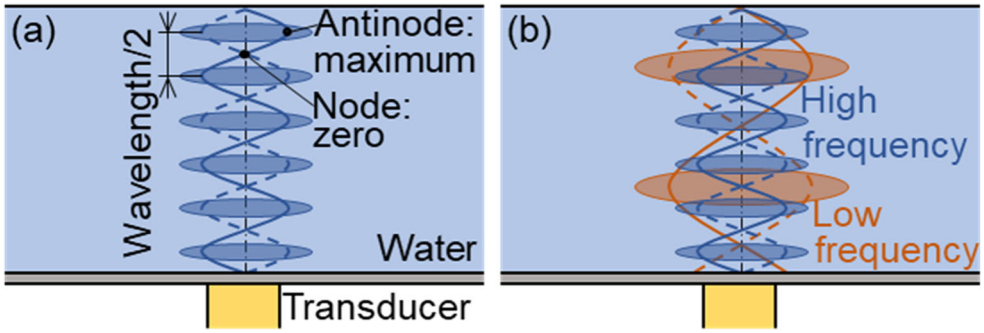

Fig. 1 Ultrasonic waves in **a** single- and **b** dual-frequencies ultrasonic cleaning

of the solution and water were 40 °C. The width and length of the cleaned specimens were both 50 mm. Water cleaning and observation with the naked eye were repeated every 0.5 min of ultrasonic cleaning until the oxide scale was completely removed.

2.3 Specimen used for ultrasonic cleaning

Uncoated 22MnB5 steel sheets having a thickness of 1.6 mm were heated in a furnace keeping a temperature of 930 °C for 170 s. The heated sheets were transferred from the furnace for about 10 s and were die-quenched between upper and lower flat dies under a contact pressure of 10 MPa for 20 s without forming. Since the martensite transformation for the 22MnB5 sheets occurs for a cooling rate above 30 °C/s and the time during die quenching is very short, the effect of the cooling rate on the oxidation is small. The degree of oxidation in furnace heating was reduced by fuel-rich combustion [35]. The Vickers hardness of the quenched sheets was about 510 HV1. The specimens were laser-cut from the quenched sheet. The surface and the cross section near the surface of the specimen are shown in Fig. 3. The oxide scale was almost uniformly formed on both surfaces of the specimen. The oxide scale thickness was about 5 μm and was comparatively thin due to the fuel-rich combustion.

3 Results of ultrasonic cleaning of hot-stamped sheets

3.1 Effect of diluted phosphoric acid solution

The effect of the diluted phosphoric acid solution on the removal of the oxide scale was examined from a comparison with a diluted hydrochloric acid solution. The temperatures of both solutions were 40 °C. The removing times t for the phosphoric and hydrochloric acid solutions for pH 1 and 2 and the single high frequency of f = 0% are shown in Fig. 4. The removing time is the time for completely removing the oxide scale. The removing time for pH 2 is longer than that for pH 1, and the oxide scale was not completely removed for 60 min by the hydrochloric acid solution of pH 2. The removing time for the phosphoric acid solution is shorter than that for the hydrochloric acid solution. Although the removing time decreases with increasing solution temperature, the temperature for the hydrochloric acid solution is limited below 40 °C because of remarkable evaporation. For the phosphoric acid solution, the applicable temperature is higher due to nonvolatility.

To examine the effect of the phosphoric and hydrochloric acids on the corrosion, the ultrasonic-cleaned specimens for pH 1 and f = 0% shown in Fig. 4 were left without water cleaning for 5 min, as shown in Fig. 5. The red rust appeared on the surface of the specimen for the hydrochloric acid,

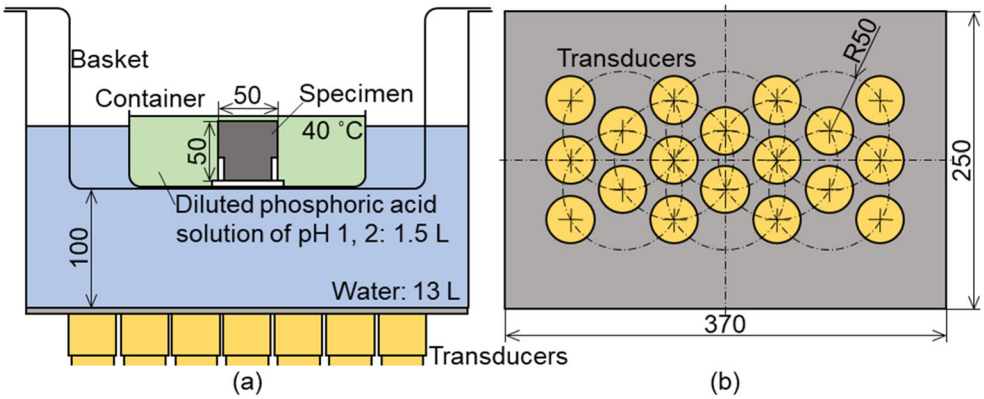

Fig. 2 Conditions of ultrasonic cleaning with diluted phosphoric acid solution. **a** Front view. **b** Top view

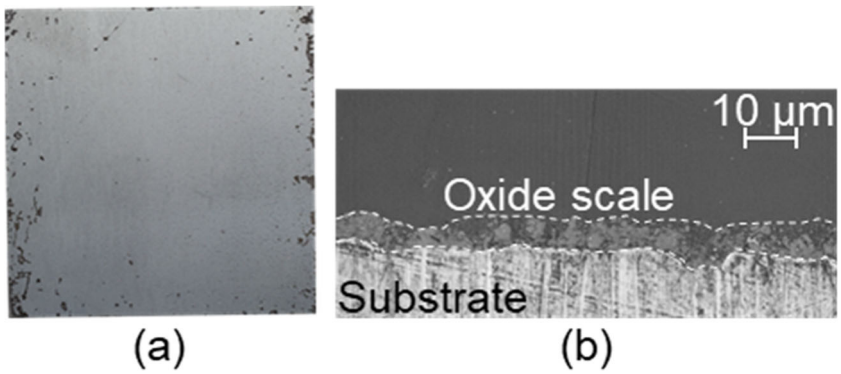

Fig. 3 **a** Surface and **b** cross section near surface of specimen

whereas no rust appeared for the phosphoric acid due to the formation of an iron phosphate layer on the surface [30]. The phosphoric acid has a function for preventing the occurrence of the rust. It was found that the phosphoric acid solution is more useful to remove the oxide scale of the hot-stamped parts than the hydrochloric acid solution.

3.2 Effect of dual-frequency ultrasonic cleaning

The removing behaviors of the oxide scale during ultrasonic cleaning with the diluted phosphoric acid solution were taken with an underwater camera, as shown in Fig. 6. Bubbles induced by ultrasonic cleaning are shown, because the photographs were taken with the underwater camera. For the single high frequency of f = 0%, the oxide scale is nonuniformly removed by the nonuniform pressure distribution, and thus the removing time becomes longer, t = 3 min. By mixing the low and high frequencies for f = 50%, the nonuniformity of the pressure distribution is improved, and the removing time is largely shortened to t = 1 min.

The relationships between the removing time and the low frequency percentage for pH 1 and 2 are illustrated in Fig. 7. The removing time sharply decreases with increasing low frequency percentage and is almost constant above f = 17%.

Although the dissolution rate for the phosphoric acid solution increases with increasing temperature [36], the cavitation intensity decreases with increasing temperature [37]. To examine the effect of the cleaning solution temperature on the removing time, the solution temperature was varied between 25 and 60 °C. The relationships between the removing time and the solution temperature for pH 1 and 2 and f = 50% are shown in Fig. 8. As the solution temperature increases, the removing time decreases. The removing time for pH 1 is saturated above a solution temperature of 40 °C.

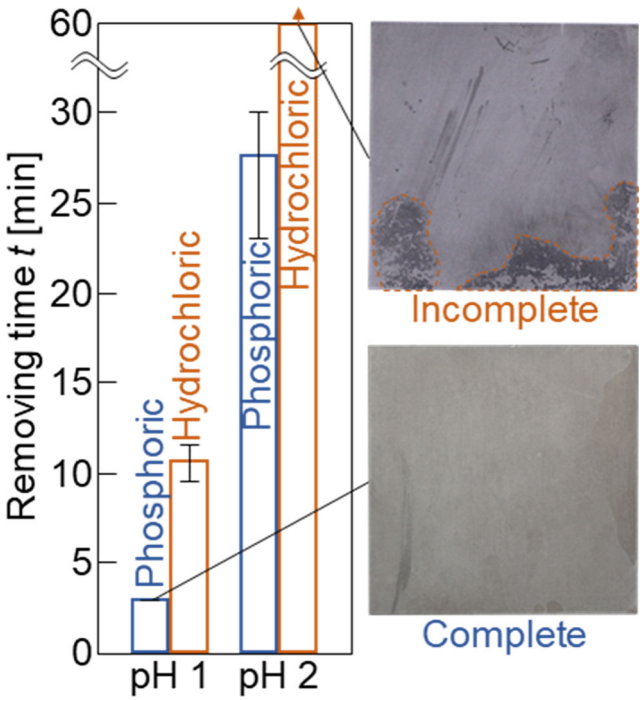

Fig. 4 Removing times for phosphoric and hydrochloric acid solutions for pH 1 and 2 and f = 0%

3.3 Effect of oxide scale thickness

To examine the effect of the oxide scale thickness on the removal of the oxide scale, resistance heating and furnace heating without fuel-rich combustion were added. Uncoated 22MnB5 steel sheets having a thickness of 0.8 mm were

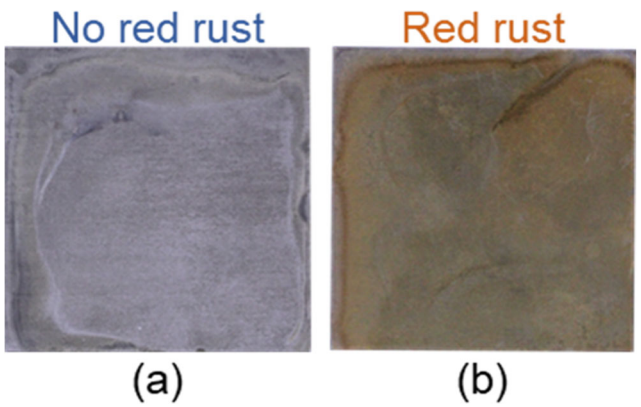

Fig. 5 Ultrasonic-cleaned specimens with **a** phosphoric and **b** hydrochloric acid solutions of pH 1 left without water cleaning for 5 min

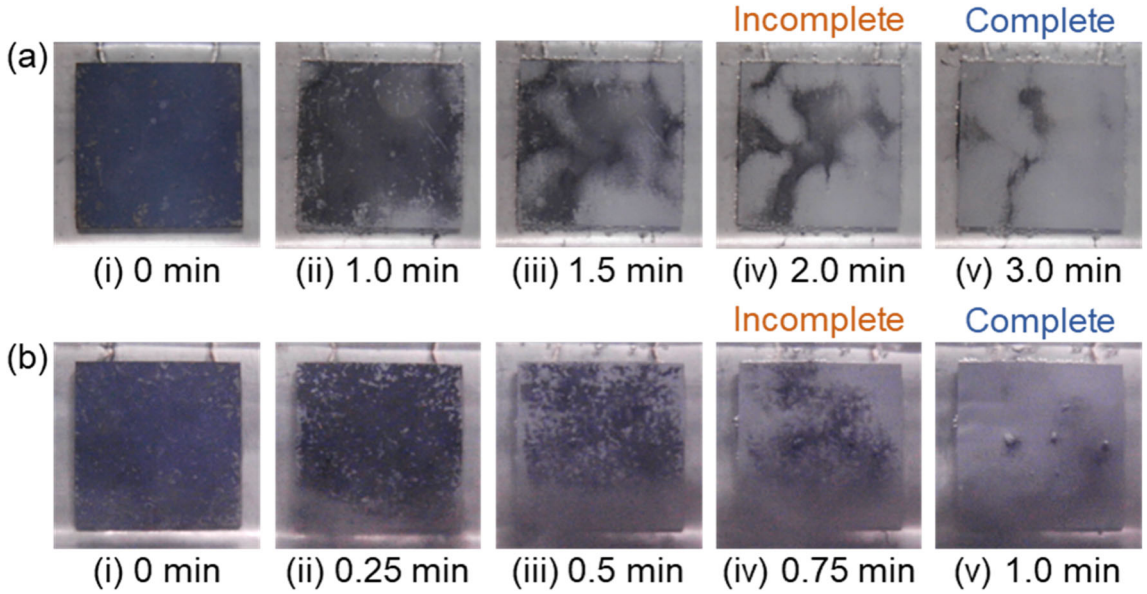

Fig. 6 Removing behaviors of oxide scale during single- and dual-frequencies ultrasonic cleaning for pH 1 and f = **a** 0 and **b** 50%

resistance-heated to 915 °C for 12.5 s. The sheets having a thickness of 1.6 mm were heated in a furnace keeping a temperature of 930 °C for 180 s. The hardness of the quenched sheets for resistance and furnace heating was about 540 and 500 HV1, respectively. The cross sections near the surface of the specimens by resistance heating and furnace heating without fuel-rich combustion are shown in Fig. 9. The oxide scale thicknesses for resistance heating and furnace heating without fuel-rich combustion were about 13 and 41 μm, respectively, and are thicker than that for furnace heating with fuel-rich combustion shown in Fig. 3.

The oxide scales of the specimens by resistance heating and furnace heating without fuel-rich combustion were removed by ultrasonic cleaning with the diluted phosphoric acid solution, as shown in Fig. 10. The removing times are longer than that for furnace heating with fuel-rich combustion shown in Fig. 6.

The relationships between the removing time and the oxide scale thickness for pH 1 and f = 0 and 50% are given in Fig. 11. The results for resistance heating and furnace heating with and without fuel-rich combustion are used. The removing time increases with increasing oxide scale thickness. The increase in removing time is considerably relieved by the dual frequency of f = 50%.

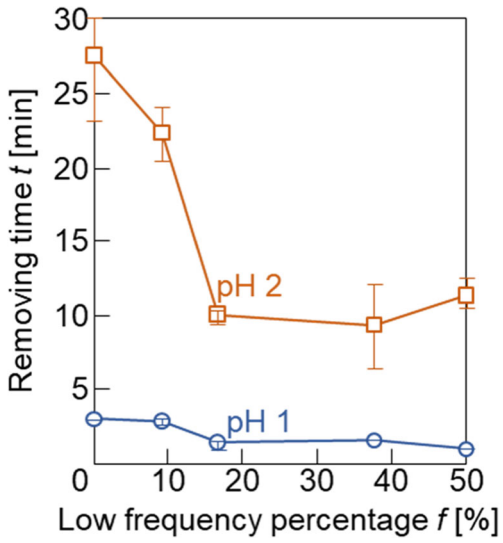

Fig. 7 Relationships between removing time and low frequency percentage for pH 1 and 2

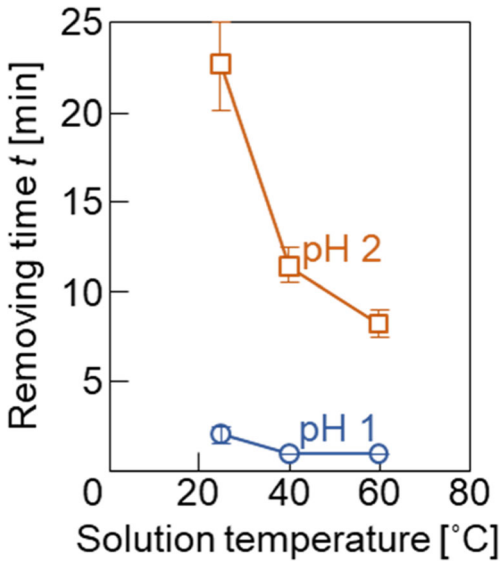

Fig. 8 Relationships between removing time and solution temperature for pH 1 and 2 and f = 50%

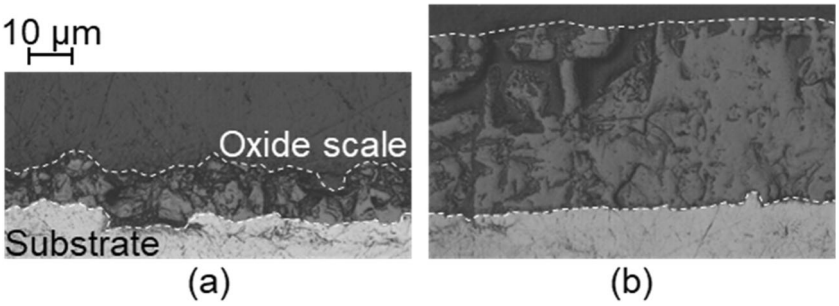

Fig. 9 Cross sections near surface of specimens by **a** resistance heating and **b** furnace heating without fuel-rich combustion

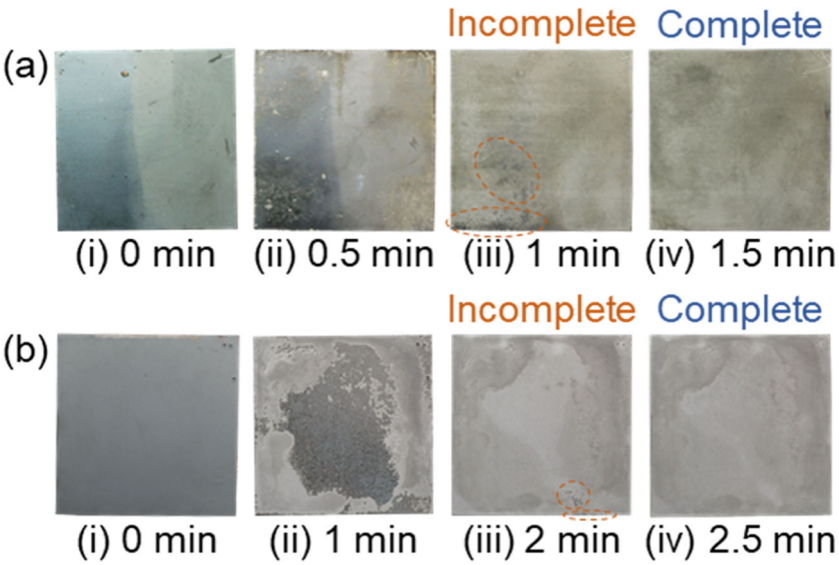

Fig. 10 Removing behaviors of oxide scale of specimens by **a** resistance heating and **b** furnace heating without fuel-rich combustion for pH 1 and $f = 50\%$

4 Results of ultrasonic cleaning of hot-stamped part

Dual-frequency ultrasonic cleaning with the diluted phosphoric acid solution was applied to remove the oxide scale of a hot-stamped part. An uncoated 22MnB5 steel sheet having a thickness of 1.0 mm was heated in a furnace keeping a temperature of 930 °C for 240 s. The heated sheet was transferred to forming dies for about 10 s and was hot-stamped into a door impact beam. The degree of oxidation in furnace heating was reduced by fuel-rich combustion. The door impact beam was cut to a length of 50 mm, and the hardness was about 500 HV1. The cut door impact beam and the distribution of oxide scale thickness are given in Fig. 12. The cut door impact beam was placed in the position of the specimen in Fig. 2 with the flanges down. Although the whole surface of the hot-stamped part is oxidized, the distribution of oxide scale thickness is nonuniform due to forming. In the flat portions of A, E, and I, the oxide scale thickness is about 10 μm, and the difference between the upper and lower surfaces is small. Around the corners of B, D, F, and H, the oxide scale thickness of the inside is thicker than that of the outside due to the compressive deformation.

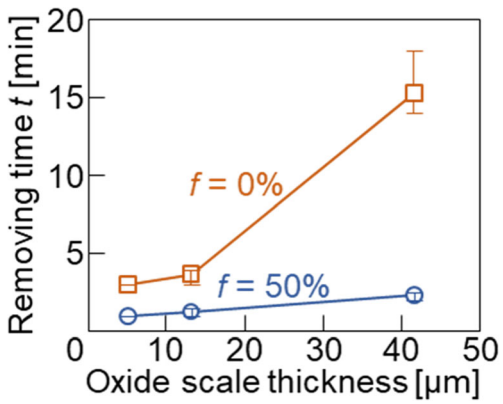

Fig. 11 Relationships between removing time and oxide scale thickness for pH 1 and $f = 0$ and 50%

The removing behavior of the oxide scale of the cut door impact beam for pH 1 and $f = 50\%$ is shown in Fig. 13. The time for completely removing the oxide scales in the inside corners, middle bottom, and sidewalls becomes longer. The removing time for pH 1 and $f = 50\%$ was $t = 1.5$ min, whereas that for pH 1 and $f = 0\%$ was $t = 3$ min.

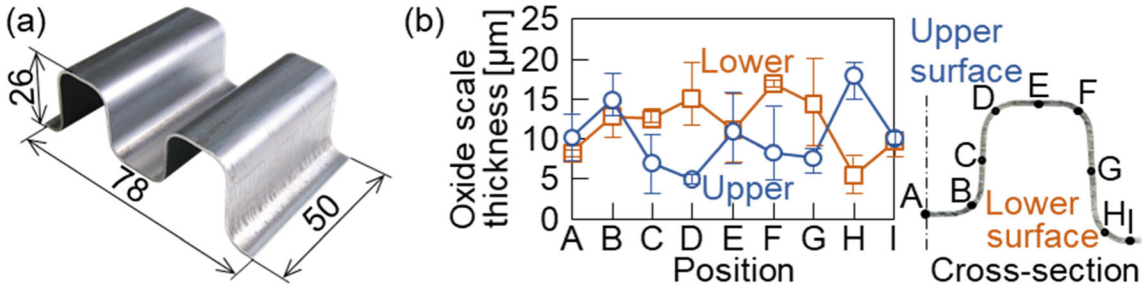

Fig. 12 **a** Cut door impact beam and **b** distribution of oxide scale thickness

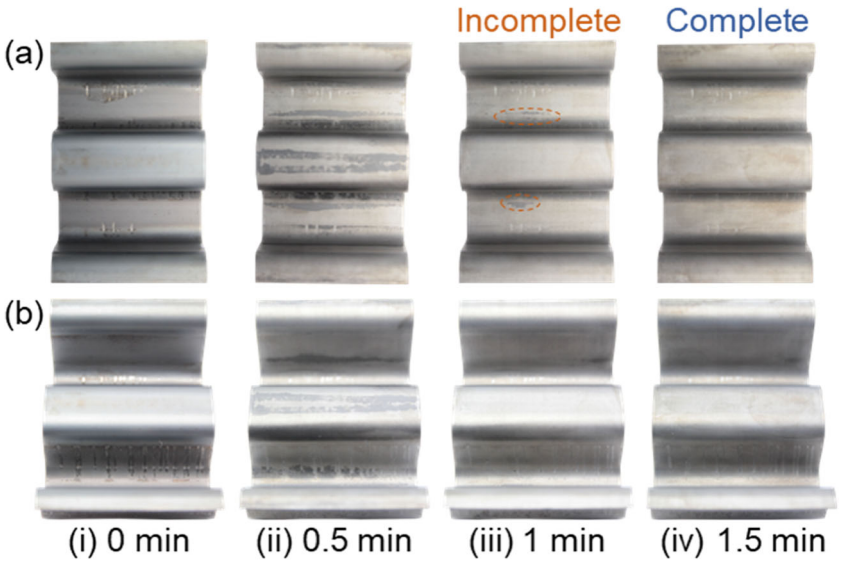

Fig. 13 Removing behavior of oxide scale of cut door impact beam for pH 1 and $f = 50\%$. **a** Lower view. **b** Lower side view

The surface and the change in angle of the outer sidewall of the door impact beam for ultrasonic cleaning for pH 1 and $f = 50\%$ are compared with those for shot blasting in Fig. 14. The surface for ultrasonic cleaning is smoother than that for shot blasting, and the change in angle is smaller.

5 Discussion

5.1 Removing mechanism of oxide scale

The removing mechanism of the oxide scale by dual-frequency ultrasonic cleaning with the diluted phosphoric acid

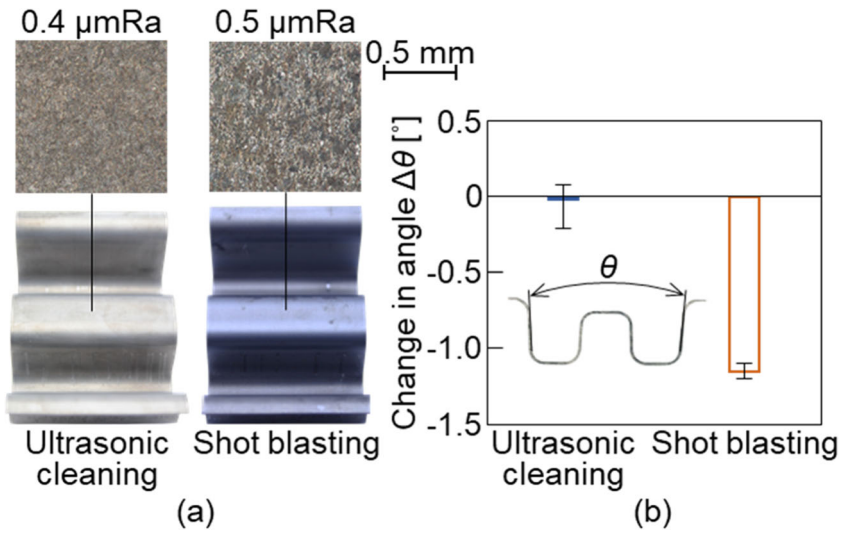

Fig. 14 **a** Surfaces and **b** changes in angle of outer sidewall of door impact beam for ultrasonic cleaning for pH 1 and $f = 50\%$ and shot blasting

solution was investigated. The effects of dual-frequency ultrasonic cleaning and the phosphoric acid solution on the removing behaviors of the oxide scale are shown in Fig. 15. Without ultrasonic cleaning, the removing time was $t = 6.5$ min, whereas the oxide scale could not be completely removed even for 30 min without the phosphoric acid; i.e., the effect of the phosphoric acid solution is larger than that of dual-frequency ultrasonic cleaning.

The relationship between the area percentage of the oxide scale and the cleaning time is given in Fig. 16. In only ultrasonic cleaning without the phosphoric acid solution, the oxide scale is gradually removed by the high pressure, whereas the complete removal is not attained. On the other hand, in only the phosphoric acid solution without ultrasonic cleaning, the oxide scale is mainly dissolved in the early stage of cleaning because of the small reduction in the area percentage, and then the removal is accelerated. The synergy effect of dual-frequency ultrasonic cleaning and the phosphoric acid solution on the removal of the oxide scale becomes remarkable.

The removing mechanism of the oxide scale in dual-frequency ultrasonic cleaning with the diluted phosphoric acid solution is illustrated in Fig. 17. In the early stage of cleaning, the dissolution of the oxide scale by the phosphoric acid solution and the acceleration of the dissolution by ultrasonic cleaning occur, and thus the oxide scale thickness decreases. Then, the oxide scales are exfoliated from the thin scale and high-pressure portions. In addition, the exfoliation starts from defects such as cracks and pores caused in the oxide scale during hot stamping [38]. The oxide scale is completely removed by both dissolution and exfoliation.

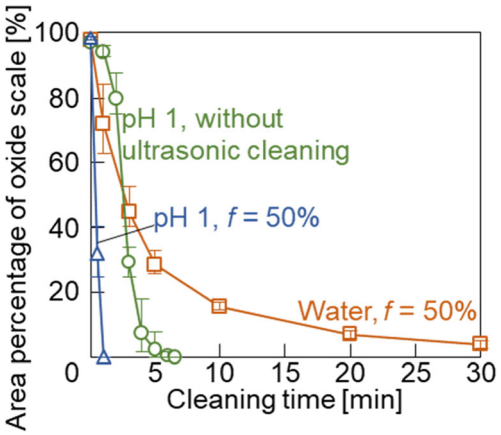

Fig. 16 Relationship between area percentage of oxide scale and cleaning time

5.2 Evaluation of weldability and paintability

To evaluate the weldability of the ultrasonic-cleaned sheets, hot-stamped 22MnB5 steel sheets from uncoated sheets having a thickness of 1.6 mm were resistance-spot welded with uncoated 980 MPa ultrahigh-strength steel sheets having a thickness of 1.6 mm, as shown in Fig. 18. The current was 9.1 kA, the passing time was 0.5 s, and the electrode force was 3.7 kN. The welded sheets were laser-cut to 100 and 30 mm in the length and width, respectively.

The nugget diameters for ultrasonic cleaning for pH 1 and f = 50%, shot blasting, and no removal of the oxide scale are given in Fig. 19. Although the nugget diameters for the three conditions are similar, the variation for no removal of the oxide scale is large.

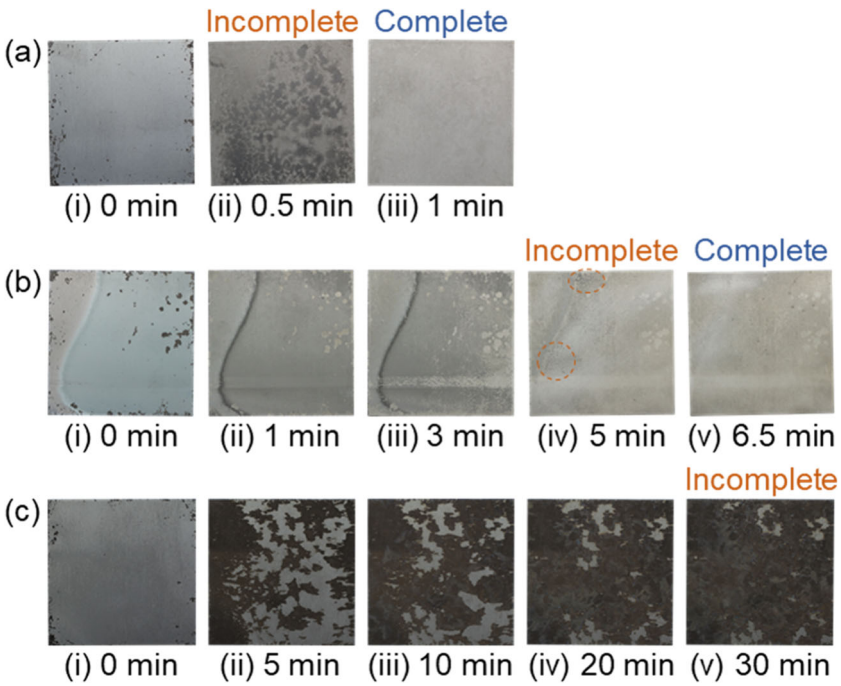

Fig. 15 Removing behaviors of oxide scale for **a** pH 1 and f = 50%, **b** pH 1 and without ultrasonic cleaning, and **c** water and f = 50%

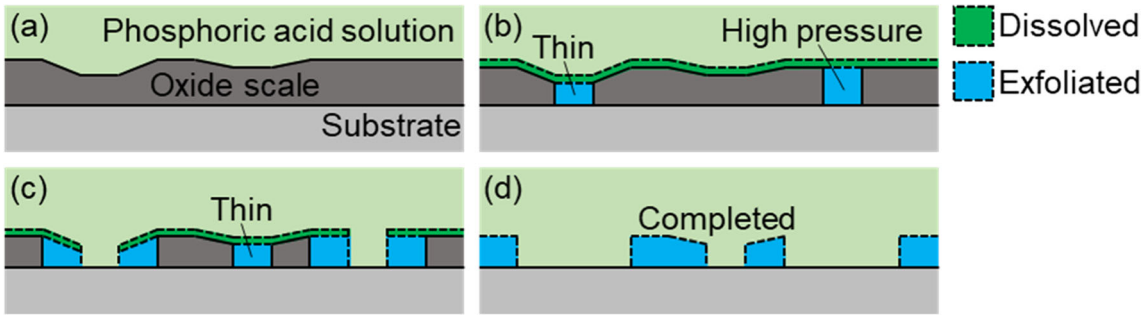

Fig. 17 Removing mechanism of oxide scale in dual-frequency ultrasonic cleaning with diluted phosphoric acid solution. **a** Before cleaning. **b** Early stage. **c** Intermediate stage. **d** Final stage

The maximum loads in the tension shearing test of the resistance-spot welded sheets for ultrasonic cleaning for pH 1 and $f = 50\%$, shot blasting, and no removal of the oxide scale are shown in Fig. 20. The maximum loads for ultrasonic cleaning and shot blasting are almost similar, and the failures of the weld are pullout modes. On the other hand, the maximum load for no removal of the oxide scale is small, and the interfacial failure of the weld is caused.

The paintability of electrodeposition coating for the ultrasonic-cleaned sheets was evaluated from the crosscut and salt spray tests. Hot-stamped 22MnB5 steel sheets from uncoated sheets were electrodeposition-coated after ultrasonic cleaning and shot blasting. In the crosscut test, the painted surface was cut into a 10 × 10 grid by a cutter, and the cut painted surface was peeled with an adhesive tape. In the salt spray test, the painted surface was cut into a cross by the cutter, and the cut surface was corroded under a salt spray environment of 5% NaCl at 35 °C for 480 h. The results of the crosscut and salt spray tests of the electrodeposition-coated sheets for ultrasonic cleaning for pH 1 and $f = 50\%$ and shot blasting are shown in Fig. 21. No flaked coating was detached from the crosscut tests for ultrasonic cleaning and shot blasting. In the salt spray test, no obvious blister and delamination of the coating around the cut portions were observed for both ultrasonic cleaning and shot blasting. It was found that the weldability and paintability for ultrasonic cleaning are similar to those for shot blasting.

5.3 Diffused hydrogen

Since the hot-stamped parts have a tensile strength of about 1500 MPa, the risk of the hydrogen-induced embrittlement is high. The amount of hydrogen diffused by dual-frequency ultrasonic cleaning with the diluted phosphoric acid solution was measured by a thermal desorption spectroscopy. The relationship between the amount of hydrogen and the cleaning time is illustrated in Fig. 22. The amount of hydrogen for pH 1 is larger than that for pH 2, and the amount for ultrasonic cleaning with water is almost constant. Although the amount of hydrogen with the phosphoric acid solution increases with increasing cleaning time, the amount is comparatively small. The solution of pH 1 is effective rather than that of pH 2 due to the short removing time.

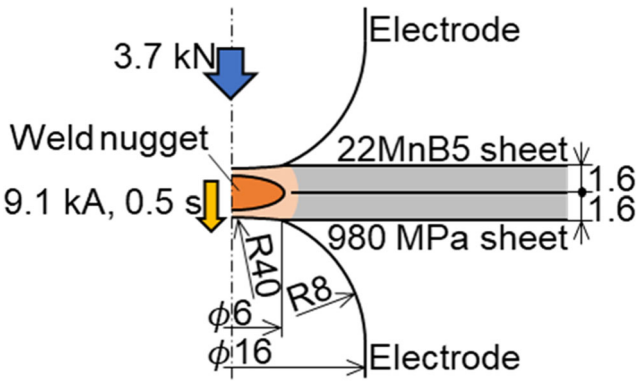

Fig. 18 Conditions of resistance-spot welding of hot-stamped 22MnB5 and 980 MPa steel sheets

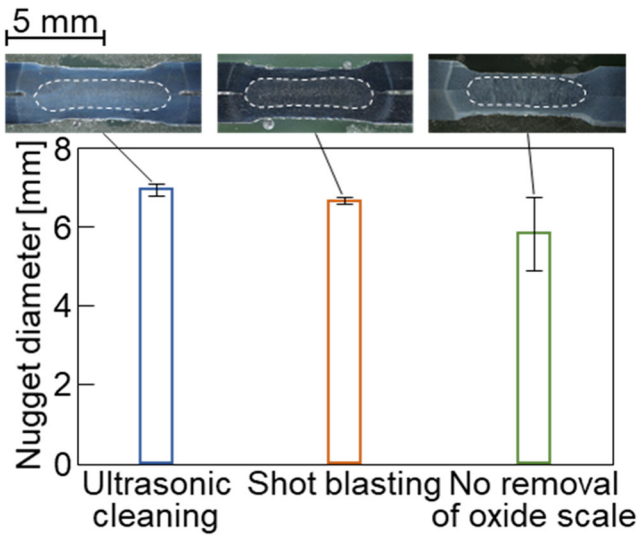

Fig. 19 Nugget diameters for ultrasonic cleaning for pH 1 and $f = 50\%$, shot blasting, and no removal of oxide scale

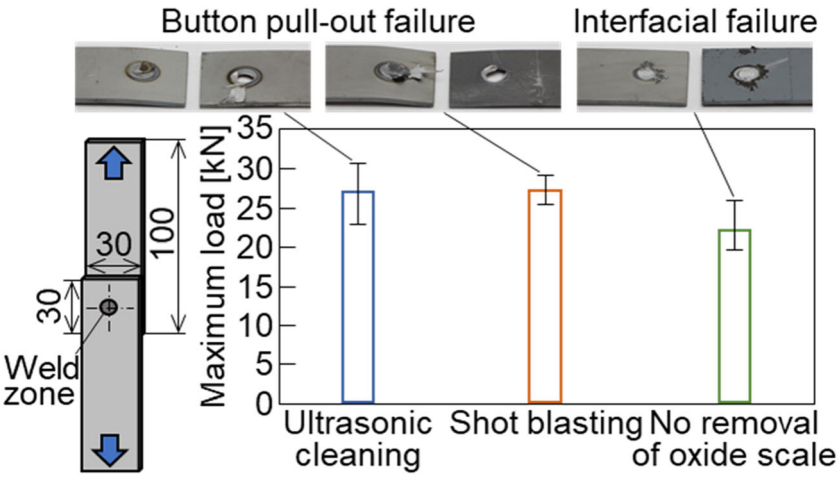

Fig. 20 Maximum loads in tension shearing test of resistance-spot welded sheets for ultrasonic cleaning for pH 1 and $f = 50\%$, shot blasting, and no removal of oxide scale

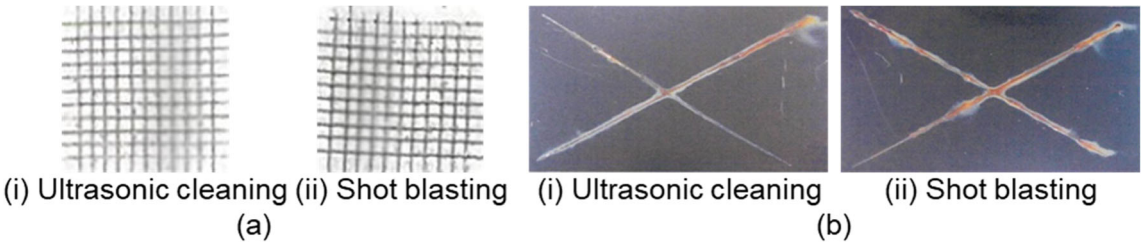

Fig. 21 The results of **a** crosscut and **b** salt spray tests of electrodeposition-coated sheets for ultrasonic cleaning for pH 1 and $f = 50\%$ and shot blasting

6 Conclusions

Hot stamping of uncoated steel sheets has the advantages of a short heating time and low material cost. Although the oxide scale formed in hot stamping of the uncoated sheets is generally removed by shot blasting to attain high weldability and paintability, produced parts have rough surface and distortion. In the present study, dual-frequency ultrasonic cleaning with the diluted phosphoric acid solution was developed to remove the oxide scale of the uncoated sheets in hot stamping, and the obtained results are summarized as follows:

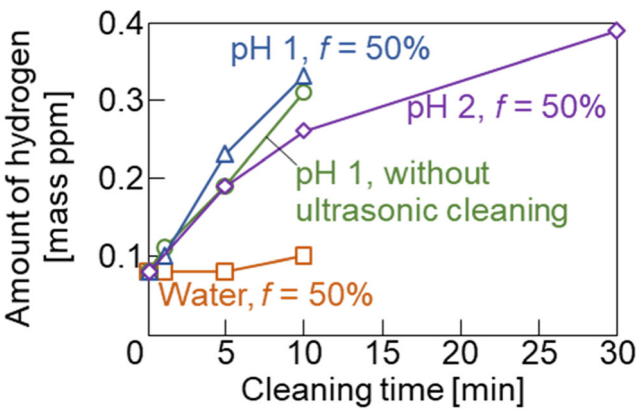

Fig. 22 Relationship between amount of hydrogen and cleaning time

1) The time for completely removing the oxide scale is greatly shortened by the dual frequency of ultrasonic cleaning with the diluted phosphoric acid solution.
2) The dissolution of the oxide scale by the phosphoric acid solution and the acceleration of the dissolution by ultrasonic cleaning early occur, and the oxide scales are exfoliated from the thin scale and high-pressure portions.
3) The removing time becomes shorter with decreasing pH and oxide scale thickness and with increasing solution temperature.
4) The surface roughness and distortion of the ultrasonic-cleaned hot-stamped part are improved in comparison with shot blasting, and the weldability and paintability are similar.
5) The removing time for the phosphoric acid solution is shorter than that for the hydrochloric acid solution, and rust of the ultrasonic-cleaned parts is prevented.

The developed process is to mix the mechanical treatment of dual-frequency ultrasonic cleaning and the chemical treatment of the phosphoric acid solution, and the synergy effect of the two treatments attains. The removal of the oxide scale is accelerated by the dissolution using the acid and the exfoliation using the pressure. Since the hot-stamped parts are generally cleaned before electrodeposition coating, conventional shot blasting processes can be omitted by replacing conventional cleaning processes with the present ultrasonic cleaning

process. Although the present process was developed to remove the oxide scale of the uncoated sheets in hot stamping, it is applicable to remove oxide scales of hot-forged parts, welded parts, etc. The dual frequency is attractive in heightening cleaning functions.

Funding This work was supported by JSPS KAKENHI Grant-in-Aid for Scientific Research (B) of Number JP18H01749.

Data availability The data that support the findings of this study are available from the corresponding author on reasonable request.

Code availability Not applicable.

Declarations

Competing interests The authors declare no competing interests.

References

1. Tisza M, Czinege I (2018) Comparative study of the application of steels and aluminium in lightweight production of automotive parts. Int J Lightweight Mater Manuf 1(4):229–238. https://doi.org/10.1016/j.ijlmm.2018.09.001
2. Mori K, Akita K, Abe Y (2007) Springback behaviour in bending of ultra-high-strength steel sheets using CNC servo press. Int J Mach Tools Manuf 47(2):321–325. https://doi.org/10.1016/j.ijmachtools.2006.03.013
3. Mishra A, Thuillier S (2014) Investigation of the rupture in tension and bending of DP980 steel sheet. Int J Mech Sci 84:171–181. https://doi.org/10.1016/j.ijmecsci.2014.04.023
4. Kim H, Han S, Yan Q, Altan T (2008) Evaluation of tool materials, coatings and lubricants in forming galvanized advanced high strength steels (AHSS). CIRP Ann Manuf Technol 57(1):299–304. https://doi.org/10.1016/j.cirp.2008.03.029
5. Mori K, Bariani PF, Behrens BA, Brosius A, Bruschi S, Maeno T, Merklein M, Yanagimoto J (2017) Hot stamping of ultra-high strength steel parts. CIRP Ann Manuf Technol 66(2):755–777. https://doi.org/10.1016/j.cirp.2017.05.007
6. Nakagawa Y, Mori K, Maeno T (2018) Springback-free mechanism in hot stamping of ultra-high-strength steel parts and deformation behaviour and quenchability for thin sheet. Int J Adv Manuf Technol 95(1-4):459–467. https://doi.org/10.1007/s00170-017-1203-3
7. Borsetto F, Ghiotti A, Bruschi S (2009) Investigation of the high strength steel Al-Si coating during hot stamping operations. Key Eng Mater 410-411:289–296. https://doi.org/10.4028/www.scientific.net/KEM.410-411.289
8. Lee CW, Fan DW, Sohn IR, Lee SJ, De Cooman BC (2012) Liquid-metal-induced embrittlement of Zn-coated hot stamping steel. Metall Mater Trans A 43(13):5122–5127. https://doi.org/10.1007/s11661-012-1316-0
9. Lehmann H (2011) Developments in the field of schwartz heat treatment furnaces for press hardening industry. Proceedings of 3rd International Conference on Hot Sheet Metal Forming of High-Performance Steel:171–179.
10. Mori K, Maki S, Tanaka Y (2005) Warm and hot stamping of ultra high tensile strength steel sheets using resistance heating. CIRP Ann Manuf Technol 54(1):209–212. https://doi.org/10.1016/S0007-8506(07)60085-7
11. Kolleck R, Veit R, Merklein M, Lechler J, Geiger M (2009) Investigation on induction heating for hot stamping of boron alloyed steels. CIRP Ann Manuf Technol 58(1):275–278. https://doi.org/10.1016/j.cirp.2009.03.090
12. Hubberstey S (2020) Perfecting a projection weld in ultrahigh-strength steel. The Fabricator. https://www.thefabricator.com/thefabricator/article/assembly/perfecting-a-projection-weld-in-ultrahigh-strength-steel
13. Yao Z, Ma F, Liu Q, Zhao F, Li F, Lin J, Wang X, Song W (2013) High temperature oxidation resistance and mechanical properties of uncoated ultrahigh-strength steel 22MnB5. Lect Notes Electr Eng 199(11):67–78. https://doi.org/10.1007/978-3-642-33747-5_7
14. Dvorak B, Tawk J (2017) Advancements in furnace design improve hot stamping. Stamp J. https://www.thefabricator.com/stampingjournal/article/stamping/advancements-in-furnace-design-improve-hot-stamping
15. Zhang S, Huang Y, Sun B, Liao Q, Lu H, Jian B, Mohrbacher H, Zhang W, Guo A, Zhang Y (2015) Effect of Nb on hydrogen-induced delayed fracture in high strength hot stamping steels. Mater Sci Eng A 626:136–143. https://doi.org/10.1016/j.msea.2014.12.051
16. Billur E, Son HS (2018) Blank materials. In: Billur E (ed) Hot stamping of ultra high-strength steels. Springer Nature, Switzerland AG, pp 45–76. https://doi.org/10.1007/978-3-319-98870-2_4
17. Mori K, Ito D (2009) Prevention of oxidation in hot stamping of quenchable steel sheet by oxidation preventive oil. CIRP Ann Manuf Technol 58(1):267–270. https://doi.org/10.1016/j.cirp.2009.03.055
18. Fan DW, De Cooman BC (2012) State-of-the-knowledge on coating systems for hot stamped parts. Steel Res Int 83(5):412–433. https://doi.org/10.1002/srin.201100292
19. Hikida K, Nishibata T, Kikuchi H, Suzuki T, Nakayama N (2013) Properties of new TS 1800 MPa grade hot stamping steel and application for bumper beam. Proceedings of 4th International Conference on Hot Sheet Metal Forming of High-Performance Steel:127–134.
20. Rosenstock D, Banik J, Gerber T, Myslowicki S (2019) Hot stamping steel grades with increased tensile strength and ductility - MBW-K 1900, tribond 1200 and tribond 1400. IOP Conf Ser Mater Sci Eng 651(1):012040. https://doi.org/10.1088/1757-899X/651/1/012040
21. Wang Z, Zhang Y, Zhu B, Wang Y, Ding H, Cai M (2017) Hot stamped parts with desirable properties in medium Mn TRIP steels. Procedia Eng 207:699–704. https://doi.org/10.1016/j.proeng.2017.10.1044
22. Mason TJ (2016) Ultrasonic cleaning: an historical perspective. Ultrason Sonochem 29:519–523. https://doi.org/10.1016/j.ultsonch.2015.05.004

23. Chahine GL, Kapahi A, Choi JK, Hsiao CT (2016) Modeling of surface cleaning by cavitation bubble dynamics and collapse. Ultrason Sonochem 29:528–549. https://doi.org/10.1016/j.ultsonch.2015.04.026
24. Goode BJ, Jones RD, Howells JNH (1998) Ultrasonic pickling of steel strip. Ultrasonics 36(1-5):79–88. https://doi.org/10.1016/S0041-624X(97)00078-4
25. Maeno T, Mori K, Ogihara T, Fujita T (2018) Blanking immediately after heating and ultrasonic cleaning for compact hot-stamping systems using rapid resistance heating. Int J Adv Manuf Technol 97(9-12):3827–3837. https://doi.org/10.1007/s00170-018-2232-2
26. Lazzarotto L, Maréchal C, Dubar L, Dubois A, Oudin J (1999) The effects of processing bath parameters on the quality and performance of zinc phosphate stearate coatings. Surf Coat Technol 122(2-3):94–100. https://doi.org/10.1016/S0257-8972(99)00307-2
27. Rani N, Singh AK, Alam S, Bandyopadhyay N, Denys MB (2012) Optimization of phosphate coating properties on steel sheet for superior paint performance. J Coat Technol Res 9(5):629–636. https://doi.org/10.1007/s11998-012-9395-9
28. Li G, Niu L, Lian J, Jiang Z (2004) A black phosphate coating for C1008 steel. Surf Coat Technol 176(2):215–221. https://doi.org/10.1016/S0257-8972(03)00736-9
29. Ocampo LM, Margarit ICP, Mattos OR, Córdoba-de-Torresi SI, Fragata FL (2004) Performance of rust converter based in phosphoric and tannic acids. Corros Sci 46(6):1515–1525. https://doi.org/10.1016/j.corsci.2003.09.021
30. Avdeev YG (2019) Protection of metals in phosphoric acid solutions by corrosion inhibitors. A review. Int J Corros Scale Inhib 8(4):760–798. https://doi.org/10.17675/2305-6894-2019-8-4-1
31. Kuzin AV, Gorichev IG, Lainer YA (2013) Stimulating effect of phosphate ions on the dissolution kinetics of iron oxides in an acidic medium. Russ Metall (Met) 9:652–657. https://doi.org/10.1134/S0036029513090073
32. Tangsopa W, Thongsri J (2019) Development of an industrial ultrasonic cleaning tank based on harmonic response analysis. Ultrasonics 91:68–76. https://doi.org/10.1016/j.ultras.2018.07.013
33. Krefting D, Mettin R, Lauterborn W (2004) High-speed observation of acoustic cavitation erosion in multibubble systems. Ultrason Sonochem 11(3-4):119–123. https://doi.org/10.1016/j.ultsonch.2004.01.006
34. Ye L, Zhu X, Liu Y (2019) Numerical study on dual-frequency ultrasonic enhancing cavitation effect based on bubble dynamic evolution. Ultrason Sonochem 59:104744. https://doi.org/10.1016/j.ultsonch.2019.104744
35. Schmitz N, Schneider J, Cresci E, Schwotzer C, Wünning JG, Pfeifer H (2017) Development of an energy-efficient burner for heat treatment furnaces with a reducing gas atmosphere. Proceedings of 6th International Conference on Hot Sheet Metal Forming of High-Performance Steel:57–64.
36. Benabdellah M, Hammouti B (2005) Corrosion behaviour of steel in concentrated phosphoric acid solutions. Appl Surf Sci 252(5):1657–1661. https://doi.org/10.1016/j.apsusc.2005.03.191
37. Niemczewski B (2007) Observations of water cavitation intensity under practical ultrasonic cleaning conditions. Ultrason Sonochem 14(1):13–18. https://doi.org/10.1016/j.ultsonch.2005.11.009
38. Cao G, Li Z, Tang J, Sun X, Liu Z (2017) Oxidation kinetics and spallation model of oxide scale during cooling process of low carbon microalloyed steel. High Temp Mater Process 36(9):927–935. https://doi.org/10.1515/htmp-2015-0248